THE LINK BETWEEN SOLIDIFICATION OF HIGH-TITANIA SLAG AND SUBSEQUENT COMMINUTION

Petrus Christian Pistorius
Carnegie Mellon University, USA

Hanline Kotze
Consensi Consulting, South Africa

ABSTRACT

The liquid-solid transformation of high-titania ilmenite smelter slags is of great importance in ilmenite smelting. Firstly, within the furnace a freeze lining of solidified slag is maintained to protect the furnace walls. Secondly, slag solidification after tapping appears to affect the size distribution of the crushed and milled slag; the work which is presented in this paper focuses on the link between slag solidification and subsequent comminution. Two possible links were investigated: microstructural, and thermal. The main investigated microstructural effect is that of silicates: silica and calcia are not soluble in the pseudo¬brookite phase which forms the bulk of the solidified slag; all of the silica and calcia in the slag hence form separate phases, intergranularly between the pseudobrookite. After comminution, silicates are present on the surface of the larger particles (larger than 106 μm), and liberated silicates are found in the smaller size fraction, confirming a role of the silicates. Microcracking of the pseudobrookite is a second important microstructural effect. All of the microstructures displayed substantial microcracking, which is likely to affect comminution – although the nature of this effect was not studied in this work. Possible thermal effects were studied by predicting cooling behaviour of slag ingots. Because of the large size of the ingots and the low thermal conductivity, the solidification rate is controlled by thermal conduction through the solidifying shell. While the overall solidification rate is controlled by conduction through the solidifying shell, the surface temperature is strongly affected by the cooling method; water cooling is essential to ensure a low surface temperature during ingot cooling.

INTRODUCTION

Titanium slag is produced by carbothermic reduction of ilmenite in arc furnaces; the product contains approximately 85% titanium oxide (generally expressed as TiO_2, although there is typically around 25-30% Ti_2O_3 in the slag), 10% FeO, and the balance in other oxides, mainly MnO, SiO_2, Al_2O_3, MgO and CaO [17]. The relationship between, and transition from, liquid to solid, is of particular importance within the process and also after tapping of the slag. Within the process, a freeze lining of solidified slag is used to protect the furnace refractories against the aggressive titanium slag [5]. Also, the metal bath within the furnace is at a temperature below the melting point of the slag, and it has been suggested that a continuous process of partial solidification of slag close to the metal bath, with remelting as the resulting solid pseudobrookite moves away into the slag bath, contributes to removal of Fe° from the slag, and drives the slag to its characteristic composition close to M_3O_5 (pseudobrookite) stoichiometry [23].

The slag is tapped into cup-shaped ingot moulds, typically with a capacity of 25 tons [8]; the slag ingots are cooled in the moulds for two days (with water cooling), then tipped out of the moulds and cooled further with water sprays [8], giving a total cooling time of approximately ten days [3]. This cooling process appears to have remained largely unchanged since ilmenite smelting started [14], although results of trials with much more rapid cooling by granulation have been reported recently [3].

The work presented here focuses on possible relationships between slag solidification and subsequent comminution behaviour. Comminution follows after the slag ingots have solidified and cooled, and involves crushing and roller milling [8], to yield a top size of 850 μm. The aim is a narrow product size distribution, since particles smaller than 106 μm cannot be supplied to chlorinators, and instead fetch a lower price as feedstock to the sulphate pigment process [3]. Two solidification-related effects may affect the comminution behaviour of the solidified slag, namely the solidification microstructure, and oxidation of the ingot surface during solidification.

Microstructural Effects

The microstructure of the solidified slag is dominated by the M_3O_5 (pseudobrookite) solid-solution phase, which constitutes about 90% of the slag, and contains TiO_2, Ti_2O_3, FeO, MnO, MgO, and some Al_2O_3, Cr_2O_3 and V_2O_3 in solid solution [7]. This solid solution cannot accommodate SiO_2, which – together with the CaO, K_2O and some of the Al_2O_3 in the feed – forms separate silicate phases (both crystalline and glassy) [4, 7]. Figure 1 shows a typical example of the resulting microstructure, with the silicates between the pseudobrookite needles.

The location of the silicates between the pseudobrookite needles is in line with the expected solidification path of the slag: the silicates have a high SiO_2/Al_2O_3 ratio, contain K_2O, and have a low CaO content, and hence show low-melting behaviour, in contrast with the pseudobrookite (which has a liquidus temperature of around 1600°C). This is illustrated by Figure 2, which gives the predicted solidification behaviour of a typical slag: upon cooling pseudobrookite starts forming just below 1600°C, and formation of this phase is largely complete with only 100°C of cooling; the silicates form at much lower temperatures. Rutile forms in parallel with the pseudobrookite; the presence of rutile is evident in the micrographs of Figure 1. Rutile is thought to be present in the solidified slag because of oxidation during tapping: if the liquid slag partially is oxidised (through contact with air) during tapping, the slag composition moves away from M_3O_5 stoichiometry, and rutile forms as one of the solidification products [11].

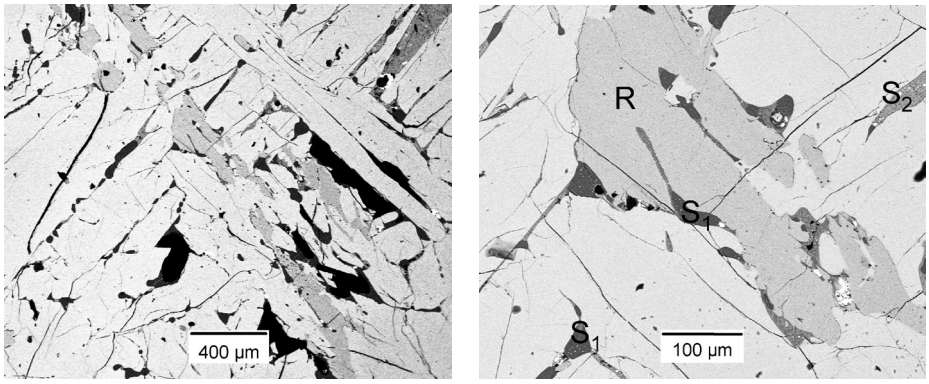

Figure 1: Typical microstructure of solidified slag [10]; backscattered electron images of the same field at two different magnifications. The light areas are pseudobrookite, the slightly darker areas rutile (labelled *R*), the dark-grey areas are silicates (labelled S_1 and S_2) and the black areas are pores.

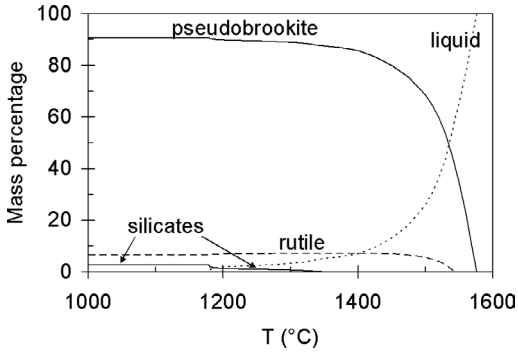

Figure 2: Predicted solidification behaviour of a slag containing 53.4% TiO_2, 31.3% Ti_2O_3, 9.7% FeO, 2.0% MnO, 1.3% SiO_2, 1.2% Al_2O_3, 0.9% MgO, 0.15% Cr_2O_3, 0.10% CaO and 0.015% K_2O. Calculated using FactSage. *Silicates* included the following crystalline phases: mullite, tridymite, anorthite and leucite.

Figure 1 shows many microcracks within the pseudobrookite, and this is characteristic of solidified titania slags. While similar cracking can result from low-temperature oxidation [2], the sample of Figure 1 was obtained (by core drilling) from the interior of a slag block, where oxidation would not have played a role. Rather, microcracking arises because of significant anisotropy of the thermal expansion coefficients, which is a characteristic of pseudobrookite: as examples, for Fe_2TiO_5 these coefficients are $\alpha a=0.6 \times 10^{-6}\ K^{-1}$, $\alpha b=10.1 \times 10^{-6}\ K^{-1}$ and $\alpha c=16.3 \times 10^{-6}\ K^{-1}$ (for the three main crystallographic directions of pseudobrookite) and for $MgTi_2O_5$ $\alpha a=2.3 \times 10^{-6}\ K^{-1}$, $\alpha b=10.8 \times 10^{-6}\ K^{-1}$ and $\alpha c=15.9 \times 10^{-6}\ K^{-1}$ [1]. Strong differences in the thermal expansion coefficients of solidified slags in the different unit cell directions were similarly demonstrated by [6] for temperatures from 323 K to 473 K.

All of these – silicates decorating the pseudobrookite grain boundaries, the presence of rutile, and microcracking – may affect particle breakdown during comminution.

Solidification and Cooling

Cooling of the slag ingots during solidification is essential to prevent decrepitation of the slag blocks [2, 8]. Decrepitation is the result of low-temperature oxidation, changing

the M_3O_5 phase to M_6O_{11}, with the resulting stress causing the material to break up into numerous small, angular particles. These particles are smaller than the 106 μm minimum for the higher-value chloride-grade slag product; decrepitation should hence be avoided, and this is done by adequately cooling the slag ingots. Decrepitation occurs at 400°C [2] and hence the surfaces of the ingots need to be cooled – by water spraying - to well below this temperature, to suppress oxidation.

If cooling took place at low Biot numbers, the convective heat transfer coefficient would have a significant effect on the rate of solidification, and hence on the microstructure of the solidified ingot. (The dimensionless Biot number is given by $Bi=hL/k$, where h is the convective heat transfer coefficient at the exterior ingot surface, L is a characteristic dimension – the radius in the case of a cylindrical ingot, and k is the thermal conductivity of the solidified slag.) Hence, at low Biot numbers (typically 1 or less) control of water spraying onto the ingot would be important to influence not only the surface temperature, but also the final microstructure; at very low Biot numbers (typically 0.1 or less) the internal temperature of the solidifying volume would be nearly uniform, and the surface temperature would be not be affected by external cooling. For large Biot numbers solidification is controlled by conduction through the solid shell, with little effect of the heat transfer coefficient on the time of solidification.

METHODOLOGY

Microstructural Effects

Milled slag samples from an industrial plant were examined, to determine whether there are differences in composition between the different particle sizes. The analyses were performed by X-ray fluorescence, with titration to determine the proportion of trivalent titanium in the slag. Milled slag was examined by electron microscopy, attaching milled slag particles to conductive (carbon) tape, and sputter coating the particles with gold; imaging by back-scattered electrons (for atomic-number contrast) and secondary electrons (for topography) was used, with EDX for micro-analysis.

Solidification and Cooling Effects

The thermal conductivity of the slag was determined by fitting a finite element model to cooling profiles measured with thermocouples embedded in pilot-scale slag ingots [10]. No details of this are presented in this paper, but the fitted thermal conductivity is used here to predict solidification times and surface temperatures of the slag ingots. These are predicted using approximate models for cylinders [18] and spheres [15]. These models apply to the classic *Stefan* problem of a material which exhibits congruent melting, and where the rate of solidification is controlled by conduction through the solid shell; the two approximate models used here are for solidification of material which is initially at the melting point, with a convective boundary condition, and assume constant thermal properties. The Stefan number, which is given by $Ste=c(T_f - T_\infty)/H_f$ (see Table 1 for explanation of the symbols), characterises cooling under such conditions. The thermal properties used in the calculations are summarised in Table 1. The heat capacity and heat of fusion of the slag were estimated using FactSage; the melting point was taken as the temperature for 50% solidification. For the values in Table 1, the Stefan number is calculated to be 2.0, which is similar to that for solidification of metals (but much larger than for the original Stefan problem of growth of ice). This means that, in this case, the heat of fusion

is approximately half as much (0.5=1/Ste) as the heat that needs to be extracted from the solid shell to cool it from the melting point to the temperature of the coolant.

Table 1: Thermal properties used in modelling

Thermal conductivity of solid slag (k)	**2 W/mK**
Heat capacity of solid slag (c)	902 J/kgK
Heat of fusion of slag (H_f)	663 kJ/kg
Density of solid slag (ρ)	3 800 kg/m^3
Melting point of slag (T_f)	1517°C
Temperature of coolant (T_∞)	30°C
Heat transfer coefficient between ingot and coolant (h)	variable; 10-1000 W/m^{2}K

The model of [18] for solidification of cylinders is based on an analytical iteration technique; an initial time is estimated, based on a zero Stefan number (that is, a very large heat of fusion); this time is then corrected for the effect of the heat capacity of the solid shell and convective cooling, by adding higher-order terms. In the results presented here, the second-order expressions of [18] were used. An advantage of this model is that it allows calculation of the surface temperature. The simplified expressions of [15] directly give the time for a given degree of solidification, for spheres with convective cooling (but do not give the surface temperature).

For both sets of calculations, the radius was taken to be 1 m, which is similar to that of industrial-sized ingots. For this radius, the Biot number hence varied from 5 (for h=10 W/m^{2}K, typical of air cooling) to 500 (for h=1000 W/m^{2}K, typical of intensive water spray cooling). These large values of the Biot number indicate that the rate of solidification is largely controlled by conduction through the solidifying shell; changes in the heat transfer coefficient are hence expected to influence the surface temperature strongly, but with little effect on the solidification time. This is indeed what the model predictions showed, as discussed below.

RESULTS AND DISCUSSION

Microstructural Effects

The detail of the relationship between microstructure and comminution is the topic of another paper [11], and hence only the main results are restated, with some additional micrographs.

There are definite differences in composition between the coarser and finer fractions of milled slag (as produced by the industrial plant); the fine particles contain nearly twice the level of CaO, SiO_2 and K_2O (that is, the oxides which report to the silicates) while the levels of FeO, MnO and MgO (oxides which report to the pseudobrookite phase) are not significantly different for the finer and coarser particles. This clearly demonstrates a link between silicates and comminution. The other prominent phase in the slag microstructure (Figure 1) is rutile, but it is not clear that this affects comminution: as Figure 3 shows, there is no significant trend in the fraction of the total titanium which is in the trivalent, with particle size. If there were a strong tendency of rutile to fracture preferentially and report to the fines, the trivalent titanium content would be expected to depend significantly on particle size (because the titanium in rutile is nearly all tetravalent), but no strong effect is observed.

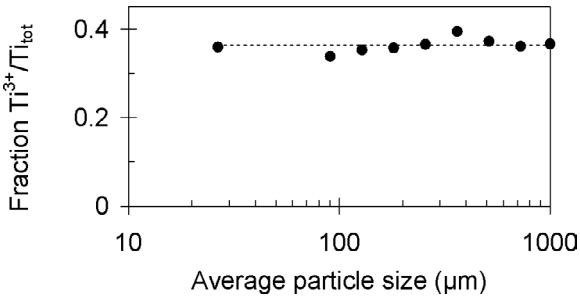

Figure 3: Lack of differences in the trivalent titanium content of particles of different sizes, for industrial milled titania slag product

The absence of a clear effect of rutile contrasts with the definite role of the silicates, as supported by the scanning electron micrographs in Figure 4. This figure shows back-scattered and secondary electron images of the +106 μm (coarser) and 106 μm (finer) size fractions of industrial milled slag. In the coarser size fraction, silicates can be observed on the surfaces of the particles; the prevalence of the silicates on the milled surface indicates that the silicates represent a preferential fracture path. In support of this, Figure 1 shows that some of the microcracks follow the interface between silicates and pseudobrookite. Preferential fracture between pseudobrookite and silicates also promotes liberation of the silicates (as small particles); this is in line with the observation of a higher silica content in the fine fraction, and the presence of liberated silicates in this fraction (see Figure 4).

Solidification and Cooling Effects

The estimated thermal conductivity of the slag – as found from the cooling profiles of pilot-scale ingots – is compared with literature data for thermal conductivity, in Figure 5. The fitted values of the thermal conductivity of the solidified slag – increasing from approximately 1 to 3 W/mK, for a temperature increase from 200°C to 1500°C – is in line with what is expected for this type of material. The main mechanism of heat conduction in these materials is phonon conductivity (diffusion of lattice vibrations), for which the expected relationship is an inverse proportionality of the thermal conductivity to absolute temperature. However, anisotropy and disorder in real structures cause deviation from this relationship [12]. The increase in the fitted slag thermal conductivity with temperature is in agreement with the observation that natural rocks which have thermal conductivities below 2 W/mK at room temperature show increases in thermal conductivity with increasing temperature [*ibid.*]. The values for the M_3O_5 materials in Figure 5 were recalculated from the reported thermal diffusivity values [20] using the average heat capacity over the range of temperatures (using enthalpies from FactSage), the room-temperature values for density [13, 21] and thermal expansion coefficients [19, 20]. The strong hysteresis in the thermal conductivity of these materials (that is, the measured values differ upon heating and cooling) was ascribed to microcracking of the material – in line with the noted anisotropy of thermal expansion of pseudobrookite. Other likely reasons for the low thermal conductivity include the relatively high molar mass of the cations in the solidified slag, and that the slag is a solid solution [9]. As with metals, solid solutions of oxides are observed to have considerably lower thermal conductivities than the pure end members [*ibid.*].

Coarse fraction

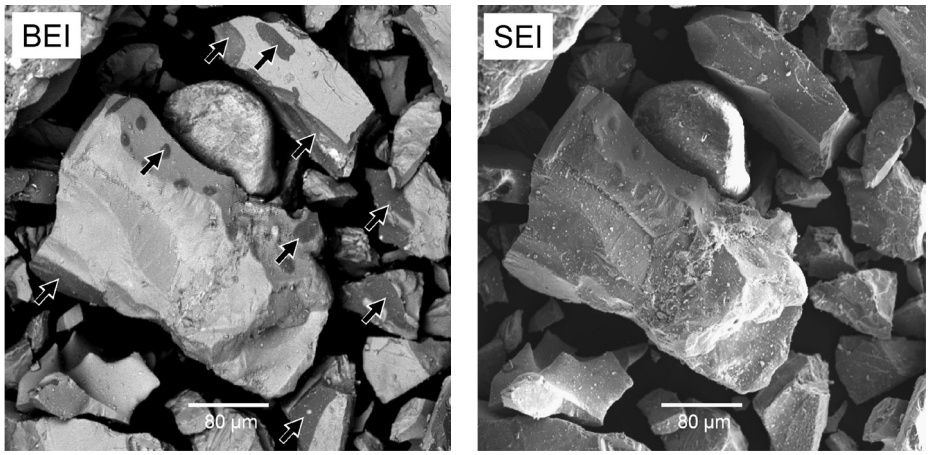

Fine fraction

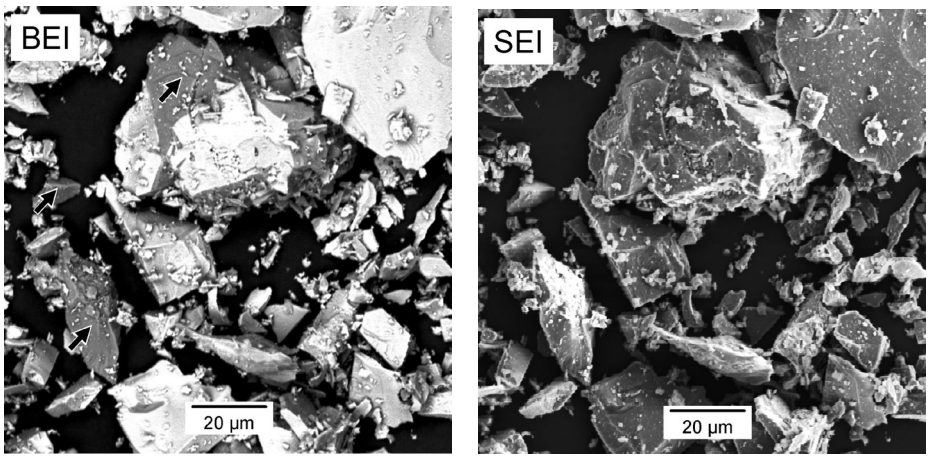

Figure 4: Scanning electron micrographs of industrial milled slag, using both back-scattered electron imaging for atomic-number contrast (images at the left, labelled *BEI*) and secondary electron imaging for topographic contrast (images at the right, labelled *SEI*). The upper pair of images is for the coarse size fraction, and the lower pair for the finer fraction. Arrowed regions are silicates (appearing darker grey in the *BEI*).

As noted earlier, the combination of a low thermal conductivity and large ingot size lead to relatively large Biot numbers, for heat transfer coefficients in the expected range of 10 to 1000 W/m^{2}K. The effects of this are evident in the model results in Figures 6 and 7. Figure 6 shows that the surface temperature of a solidifying cylinder of slag is predicted to remain well above 400°C for much of the solidification period, if normal air cooling (h=10 W/m^{2}K) is used. A tenfold increase in the heat transfer coefficient to 100 W/m^{2}K (which is readily achieved with water spray cooling) gives a sharp decrease in the surface temperature, but with little effect on the solidification time; these effects are in line with the observation that the rate of solidification is controlled by conductive heat transfer through the solidifying slag shell.

It is worth noting that the predicted solidification time is around 5-6 days, for one-dimensional cooling of cylinders, and only slightly less for spheres of the same diameter (Figure 6). This means that, at the time when the slag ingots are tipped out of the moulds (after two days of cooling) the ingots still contain a considerable fraction of liquid within the solid shell.

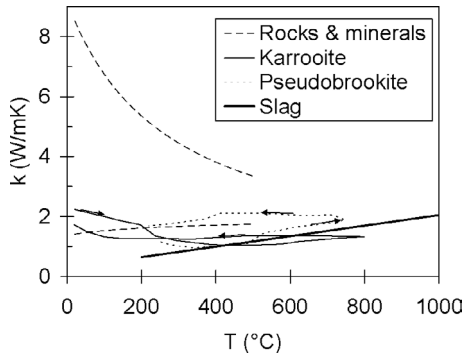

Figure 5: Comparison of the fitted thermal conductivity of the solidified slag (heavy line), with literature data on the range of thermal conductivity of natural rocks (broken line) [12], and synthetic karrooite ($MgTi_2O_5$) [20] and pseudobrookite (Fe_2TiO_5) [19]. For the M_3O_5 materials, the arrows indicate the direction of temperature change during the measurements.

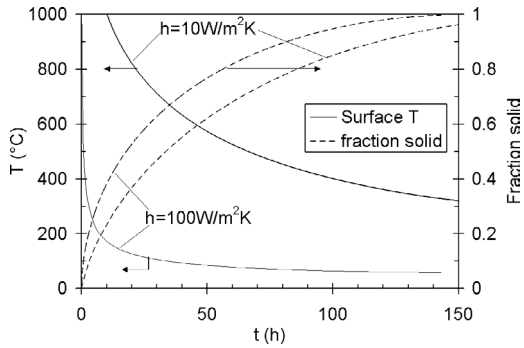

Figure 6: Solidification behaviour of slag cylinders with a radius of 1 m, for two different heat transfer coefficients to the cooling medium; predicted using the model of Shih and Tsay [18]

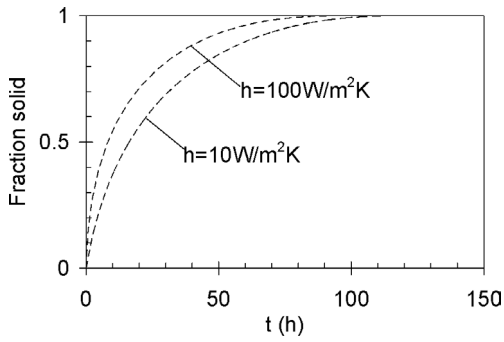

Figure 7: Solidification behaviour of slag spheres with a radius of 1 m, for two different heat transfer coefficients to the cooling medium; predicted using the expressions of Milanez [15]

CONCLUSIONS

Differences in chemical composition with particle size (of industrial milled slag) supports the suggestion that silicates have a significant effect on the milling behaviour of solidified titania slag; no strong role of rutile is evident, though. The main role of external cooling during solidification of the slag ingots is to ensure a low surface temperature (to avoid decrepitation); no strong effect of convective cooling conditions on the solidification structure and solidification time is expected.

REFERENCES

Bayer, G. (1971). Thermal Expansion Characteristics and Stability of Pseudobrookite- Type Compounds, Me_3O_5. *Journal of the Less-Common Metals*, Vol. 24, pp. 129-138. [1]

Bessinger, D., Geldenhuis, J. M. A. & Pistorius, P. C. (2005). *Phase Changes in the Decrepitation of Solidified High Titania Slags*. Heavy Minerals 2005, Jacksonville, Florida, U.S.A. Society for Mining, Metallurgy and Exploration. pp. 213-219. [2]

Bessinger, D., Beukes, P. & Glenewinkel, R. (2007). *Granulation of Titania Slag*. The 6th International Heavy Minerals Conference 'Back to Basics', Southern African Institute of Mining and Metallurgy, Johannesburg, South Africa. pp. 159-162. [3]

Borowiec, K., Grau, A. E., Guéguin, M. & Turgeon, J. F. (1998). *Method to Upgrade Titania Slag and Resulting Product*. US Patent 5,830,420. [4]

Coetzee, C., Lamont, P. H., Bessinger, D., Rabe1, J., Zietsman, J. & Muller, J. (2007). *Application of Ucar® Chill Kote™ Lining to Ilmenite Smelting*. INFACON XI Conference, New Delhi, India, February 18-21. pp. 837-846. [5]

de Villiers, J.P.R., J. Göske &A. Tuling (2005). *Disintegration in High Grade Titania Slags: low Temperature Oxidation Reactions and Associated Fracture Mechanics of Pseudobrookite*. Mineral Processing and Extractive Metallurgy, Vol. 114, pp. C73-C79. [6]

Guéguin, M. & F. Cardarelli (2007). *Chemistry and Mineralogy of Titania-rich Slags. Part 1 – Hemo-ilmenite, Sulphate, and Upgraded Titania Slags*. Mineral Processing and Extractive Metallurgy Review, Vol. 28, pp. 1-28 [7]

Gous, M. (2006). An Overview of the Namakwa Sands Ilmenite Smelting Operations. *Journal of the Southern African Institute of Mining and Metallurgy*, Vol. 106, pp. 379-384. [8]

Kingery, W. D., Bowen H. K. & Uhlmann, D. R. (1976). *Introduction to Ceramics*. Second edition. John Wiley & Sons. pp. 612-643. [9]

Kotzé, H. (2007). *Investigation into the Effect of Cooling Conditions on the Particle Size Distribution of Titania Slag*. PhD thesis, University of Pretoria. [10]

Kotzé, H. & Pistorius, P. C. (2008). *Role of Silicate Phases during Comminution of Titania Slag*. Minerals Engineering (accepted for publication). [11]

Lee, Y. & Deming, D. (1998). Evaluation of Thermal Conductivity Temperature Corrections applied in Terrestrial Heat Flow Studies. *Journal of Geophysical Research*, Vol. 103, pp. 2447-2454. [12]

Lind, M. D. & Housley, R. M. (1972). *Crystallization Studies of Lunar Igneous Rocks: Crystal Structure of Synthetic Armalcolite*. Science, Vol. 175, No. 4021, pp. 521-523. [13]

Miller, J. A. (1957). *Titanium, a Materials Survey*. United States Government Printing Office, Washington, D.C., U.S.A, p. 64. [14]

Milanez, L. F. (1985). Simplified Relations for Phase Change Process in Spherical Geometry. International, *Journal of Heat and Mass Transfer*, Vol. 28, pp. 884-885. [15]

Pistorius, P. C. (2008). Ilmenite Smelting: the Basics. *Journal of the Southern African Institute of Mining and Metallurgy*, Vol. 108, pp. 35-43. [16]

Sahu, S., Alex, T. C., Mishra, D. & Agrawal, A. (2006). *An Overview of the Production of Pigment Grade Titania from Titania-rich Slag*. Waste Management & Research, Vol. 24, pp. 74-79. [17]

Shih, Y. P. & Tsay, S. Y. (1971). *Analytical Solutions for Freezing a Saturated Liquid inside or outside Cylinders*. Chemical Engineering Science, Vol. 26, pp. 809-816. [18]

Siebeneck, H. J., Hasselman, D. P. H., Cleveland, J. J. & Bradt, R. C. (1976). Effects of Microcracking on the Thermal Diffusivity of Fe_2TiO_5. *Journal of the American Ceramic Society*, Vol. 59, pp. 241-244. [19]

Siebeneck, H. J., Hasselman, D. P. H., Cleveland J. J. & Bradt, R. C. (1977). Effects of Grain Size and Microcracking on the Thermal Diffusivity of $MgTi_2O_5$. *Journal of the American Ceramic Society*, Vol. 60, pp. 336-338. [20]

Smyth, J. R. & McCormick, T. C. (1995). *Crystallographic Data for Minerals, in Mineral Physics and Crystallography, a Handbook of Ohysical Constants*. American Geophysical Union. p. 3. [21]

Xirouchakis, D. M. (2007). *Pseudobrookite-group Oxide Solutions and Basaltic Melts*. Lithos, Vol. 85, pp. 1-9. [22]

Zietsman, J. H. & Pistorius P. C. (2004). Process Mechanisms in Ilmenite Smelting. J*ournal of the South African Institute of Mining and Metallurgy*, Vol. 104, pp. 653-660. [23]